with the crystal synthesis. The structural study of EnIV′ was supported by Grant-in-Aid for Scientific Research 242016 of the Ministry of Education of Japan. Computations were carried out on a HITAC 8800/8700 computer at the Computer Centre of the University of Tokyo.

References

COPPENS, P. & HAMILTON, W. C. (1970). *Acta Cryst.* A**26**, 71–83.

HAWTHORNE, F. C. & GRUNDY, H. D. (1977). *Can. Mineral.* **15**, 50–58.

International Tables for X-ray Crystallography (1962). Vol. III, pp. 201–209. Birmingham: Kynoch Press.

SMYTH, J. R. & ITO, J. (1977). *Am. Mineral.* **62**, 1252–1257.

TAKÉUCHI, Y., KUDOH, Y. & ITO, J. (1977). *Proc. Jpn Acad.* **53**, 60–63.

TAKÉUCHI, Y., KUDOH, Y. & ITO, J. (1984). *Acta Cryst.* B**40**, 115–125.

WUENSCH, B. J. & PREWITT, C. T. (1965). *Z. Kristallogr.* **122**, 24–59.

Acta Cryst. (1984). B**40**, 132–138

High-Resolution Electron Microscopic Studies on a New Polytype of SiC and its Intergrowth Structures

BY R. S. RAI, P. KORGUL* AND G. SINGH

Department of Physics, Banaras Hindu University, Varanasi-221005, India

(*Received* 18 *April* 1983; *accepted* 12 *October* 1983)

Abstract

Tilted-beam two-dimensional lattice images have been used to determine the structure of a new polytype of SiC, *viz* 411*R*, and its intergrowth structures. Initially, the chevron-shaped fringes in a simple structure of 6*H* were obtained and analysed with the help of computer simulation based on the multislice approach of Cowley & Moodie [*Acta Cryst.* (1957), **10**, 609–619] in order to arrive at optimum experimental conditions. The method was then applied to a high-period polytype 411*R* and its intergrowth structures. The suitability of this technique for structural investigations is discussed.

Introduction

High-resolution electron microscopy (lattice imaging) has become a powerful tool to elucidate the details at ultrastructural level which are beyond the reach of more conventional structural techniques such as X-ray diffraction (Van Landuyt, Amelinckx, Kohn & Eckart, 1974; Cowley & Iijima, 1972; Allpress & Sanders, 1973; McConnell, Hutchison & Anderson, 1974; Buseck & Iijima, 1974; Hashimoto, Endoh, Takai, Tomioka & Yokota, 1978/79; Van Tendeloo & Amelinckx, 1982, *etc.*). In SiC it is usually found that large unit cells consist of regular stackings of unit cells of one or more common structure types like 6*H*, 15*R*, 4*H* and 21*R* (Verma & Krishna, 1966; Dubey, Ram & Singh, 1973). The utility of low-resolution lattice images has already been established in the structural investigations of SiC structures of large cell parameters (Dubey & Singh, 1978; Singh & Singh, 1980; Singh, Singh & Van Tendeloo, 1981; Yessik, Shinozaki & Sato, 1975; Ogbuji, Mitchell & Heuer, 1981; Kuo, Zhou, Ye & Kuo, 1982). It has been suggested by Jepps, Smith & Page (1979) that tilted-beam two-dimensional lattice images are capable of directly revealing the stacking sequence in SiC polytype structures. Recently, Smith & O'Keefe (1983) have very critically examined the conditions for obtaining direct structure images in small-period polytypes with the help of computer simulation using Optronics Photo-Write and HREM's from the 600 kV Cambridge microscope. Their computer simulations using a variety of experimental parameters leading to a resolution limit of 0·2 nm have shown that the tetrahedral stacking can be directly recognized under very restricted imaging conditions for crystal thicknesses up to about 7·5 nm.

Computer simulation of image contrast using the multislice approach (Cowley & Moodie, 1957; Goodman & Moodie, 1974) has generally been used for confirming the inferences from the lattice images. This requires advance knowledge of the structure as well as experimental parameters like foil thickness, defocus *etc.*, some of which are not easily found. In addition, the multislice computations become too cumbersome in cases of large polytype unit cells. Therefore, the use of computer simulation in this study has been confined to a well known structure of

* Crystallography Laboratory, The University of Newcastle upon Tyne, Newcastle upon Tyne, NE1 7RU, England.

0108-7681/84/020132-07$01.50

6*H* to arrive at optimum experimental conditions. For the confirmation of structure inferred from the lattice image in a new polytype 411*R*, an alternative approach of matching the observed and calculated X-ray intensities has been adopted.

Experimental details

The structures of SiC are often found in syntactic coalescence and those of large periodicities are usually in the form of very thin lamellae so that it becomes very difficult to get even a minute piece of a crystal which is exclusively a large-period structure. Therefore, samples suitable for electron microscope examination were prepared by crushing the coalesced crystals into powder form and dispersing the tiny fragments on a holey-carbon grid. Thin flakes parallel to $\{11\bar{2}0\}$ cleavage planes were then examined on a JEM 100 CX microscope.

As all the SiC structures are built up from three-dimensional networks of tetrahedrally bonded Si and C atoms, they can be described by stacking sequences of either Si–C tetrahedra or Si–C double layers in terms of close packing of equal spheres. Fig. 1 shows a six-layered hexagonal structure (6*H*) as viewed along the *b* axis. Si or C atoms corresponding to a cyclic sequence of layers $A \rightarrow B \rightarrow C$ and those in anticyclic sequence $A \rightarrow C \rightarrow B$ lie in the tetrahedral-face planes [$(10\bar{1}2)$ and $(10\bar{1}\bar{2})$ in the 6*H* structure], which are mutually rotated by π (Jepps *et al.*, 1979). Since all the polytype structures consist of some combination of cyclic and anticyclic sequences of layers, the Si or C atoms always lie on either of the tetrahedral-face planes which are inclined equally at 109°28′ to the *c* axis. This means that the $\{10\bar{1}l\}$ and $\{10\bar{1}\bar{l}\}$ planes inclined at or very near to this angle to the *c* axis in any polytype structure have high reticular density in different parts of the unit cell depending on the layer sequence. The basal planes ($000l = \pm n$) for any *nH* or *nR* polytype also have high reticular density making these reflections invariably strong.

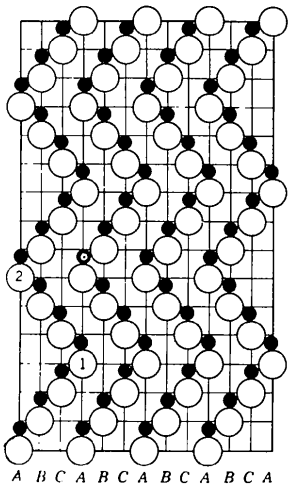

Fig. 1. Zigzag sequence of Si and C atoms in $(11\bar{2}0)$ plane of the 6*H* polytype of SiC.

In a zone-axis orientation when the incident beam is tilted to place the optic axis midway between $000l$ and $10\bar{1}l$ rows so as to allow equivalent reciprocal-lattice vectors through the aperture, crossed lattice images may be formed particularly from strong reflections of high reticular density planes. Owing to thickness variation of the sample the distribution of diffracted intensity of the allowed beams varies from one place to another giving rise to images of varying sharpness in terms of relative dominance of basal and inclined fringes. Optimum conditions are sought for which the chevron-shaped contrast resembles the projected reticular density of tetrahedral face pairs. These chevrons, along with basal fringes corresponding to individual stacking planes, may enable one to read the stacking sequence of the entire unit cell.

Two-dimensional lattice images, 6*H* SiC

Consider the structure–image correlation in the simple case of 6*H* whose structure is fully known. Fig. 2(*a*) shows a two-dimensional lattice image taken under tilted-beam illumination. The main features of the lattice image are (i) the *c*-period blocks (~1·5 nm) of 6*H* structure consisting of two parts appearing in distinct dark and light contrast. The two parts are of equal width in comparatively thinner regions (top portion of the image) while at other places respective widths vary, becoming 1 : 2 at the bottom portion; (ii) the chevron-shaped fringes in the two parts of the unit cell correspond to orientation and periodicity of $(10\bar{1}2)$ and $(10\bar{1}\bar{2})$ planes (~0·25 nm).

As can be seen from Fig. 1, each plane of the family $(10\bar{1}2)$ in one half of the unit cell and that of $(10\bar{1}\bar{2})$ in the other half consist of a closely spaced pair of silicon and carbon planes. In a crude projection along the *b* axis these pairs of Si–C atomic planes project forming chevrons of certain width which appear to bear a close correlation with the projected charge density of closely spaced Si–C atomic planes. The correlation between chevron-shaped fringes and the stacking sequence in the structure was established by multislice computations (Skarnulis, 1976) of image contrast and the match with the observed image contrast is shown (inset) in Fig. 2(*b*).

Studies on a new polytype of SiC 411*R* and its intergrowth structures

A bluish-black crystal of platelet shape (3 × 2 × 0·35 mm) having well developed basal faces was chosen from a batch of SiC crystals grown from vapour phase (Lely's method). A *c*-axis oscillation photograph of this crystal (Fig. 3) shows spots of a

137-layered polytype superimposed over a faint streak along the $10\bar{1}l$ reciprocal-lattice row. Unique identification of the polytype was not possible at this stage because spots on one side of the zero-layer line are absent due to absorption. This indicates that a high-period structure exists in a thin lamellar form on the platelet of $6H$ structure but it was not possible to isolate a smaller piece for detailed X-ray examination. The crystal was therefore crushed for detailed investigation by lattice imaging in symmetric bright-field and tilted-illumination modes.

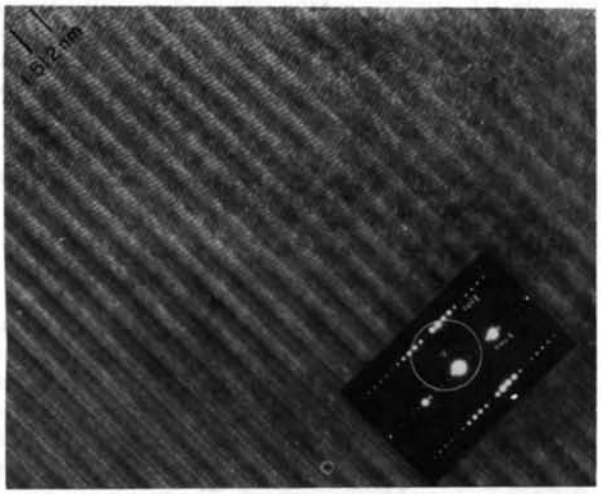

(*a*)

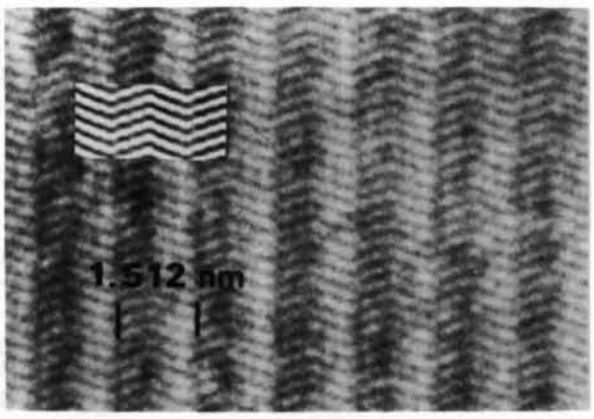

(*b*)

Fig. 2. (*a*) Tilted-beam two-dimensional lattice image of $6H$ SiC. The beam is tilted midway between $10\bar{1}l$ and $000l$ so that $10\bar{1}2$ and $10\bar{1}\bar{2}$ are included in the aperture. The inclined fringes forming chevrons are parallel to $(10\bar{1}2)$ and $(10\bar{1}\bar{2})$ planes (d spacing ~0·25 nm). In Zhdanov notation, the layer sequence read from the upper part of the image is found to be 33 while that from the lower part is not. The corresponding diffraction pattern showing the positions of the optic axis by a cross and the objective aperture by a circle is shown as inset. (*b*) Tilted-beam two-dimensional lattice image of a $6H$ SiC along with computed image (inset) (defocus value $\Delta f = -500$ Å, $C_s =$ 0·7 mm, foil thickness 30·81 Å, accelerating voltage 100 kV, depth of focus 170 Å, aperture radius 0·68 Å^{-1} and incident-beam divergence 0·001 rad).

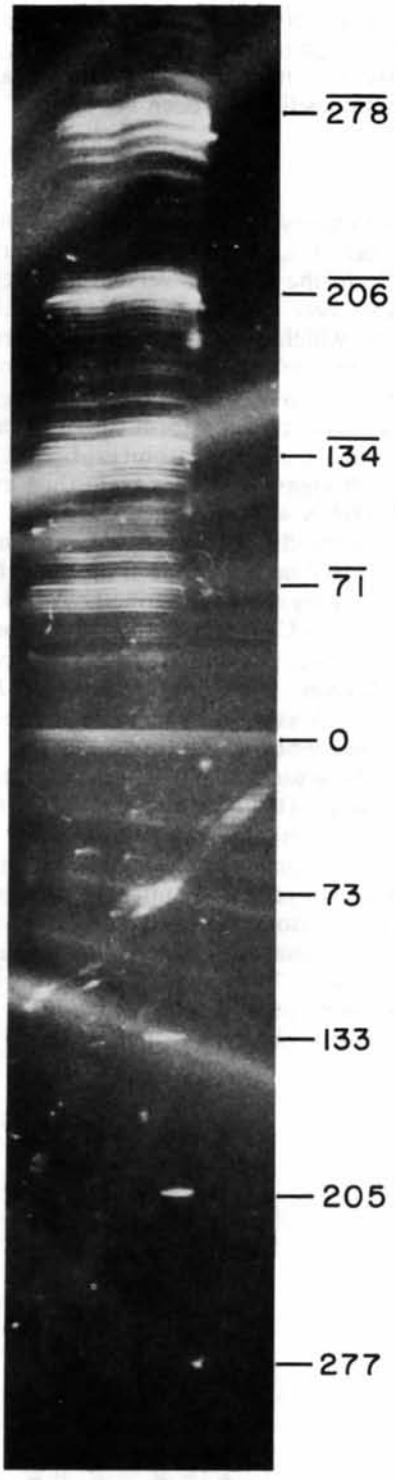

Fig. 3. The $10\bar{1}l$ reflections as recorded on a 15° c-axis oscillation photograph of the parent SiC crystal. Polytype spots superimposed over a faint streak are clearly resolved showing the periodicity of a $137H$ or $411R$ polytype. Spots on one side of the zero layer line are absent due to absorption (×6·3), Cu $K\alpha$ radiation.

Lattice imaging studies

Figs. 4(*a*), (*b*) show a bright-field lattice image and enlargement of part of it obtained from symmetrical 000*l* reflections. The lattice image reveals a superperiodicity of 145·5 nm (marked in Fig. 4). Each superperiod consists of a sequence of four blocks of smaller periods (of periodicities 34·5, 33·0, 34·5 and 43·5 nm, respectively). The same pattern of fringes was found over an extended area in the sample and Fig. 4(*a*) shows only a part of it. Most of the fringe spacings correspond to 6*H* periodicity of 1·5 nm. The four subperiods defining the superperiod arise essentially from insertion of periodic faults in a regular 6*H* matrix. The periodicity revealed by X-ray diffraction (Fig. 3) corresponds to a 34·5 nm wide subperiod in the lattice image.

Tilted-beam two-dimensional lattice images were taken under optimum conditions as in Fig. 2. Fig. 5(*b*) shows one such image of one subperiod of 34·5 nm periodicity using the encircled reflections (Fig. 5*a*). If the chevron-shaped fringes are assumed to represent the layer-stacking sequence in the structure, the stacking sequence may be expressed in Zhdanov notation as

$$32\,23\,33\,22\,23\,(33)_2\,43\,33\,32\,(33)_9\,22\,(33)_4.$$

The stacking sequence read in this fashion is not unambiguous in the sense that some of the asymmetric

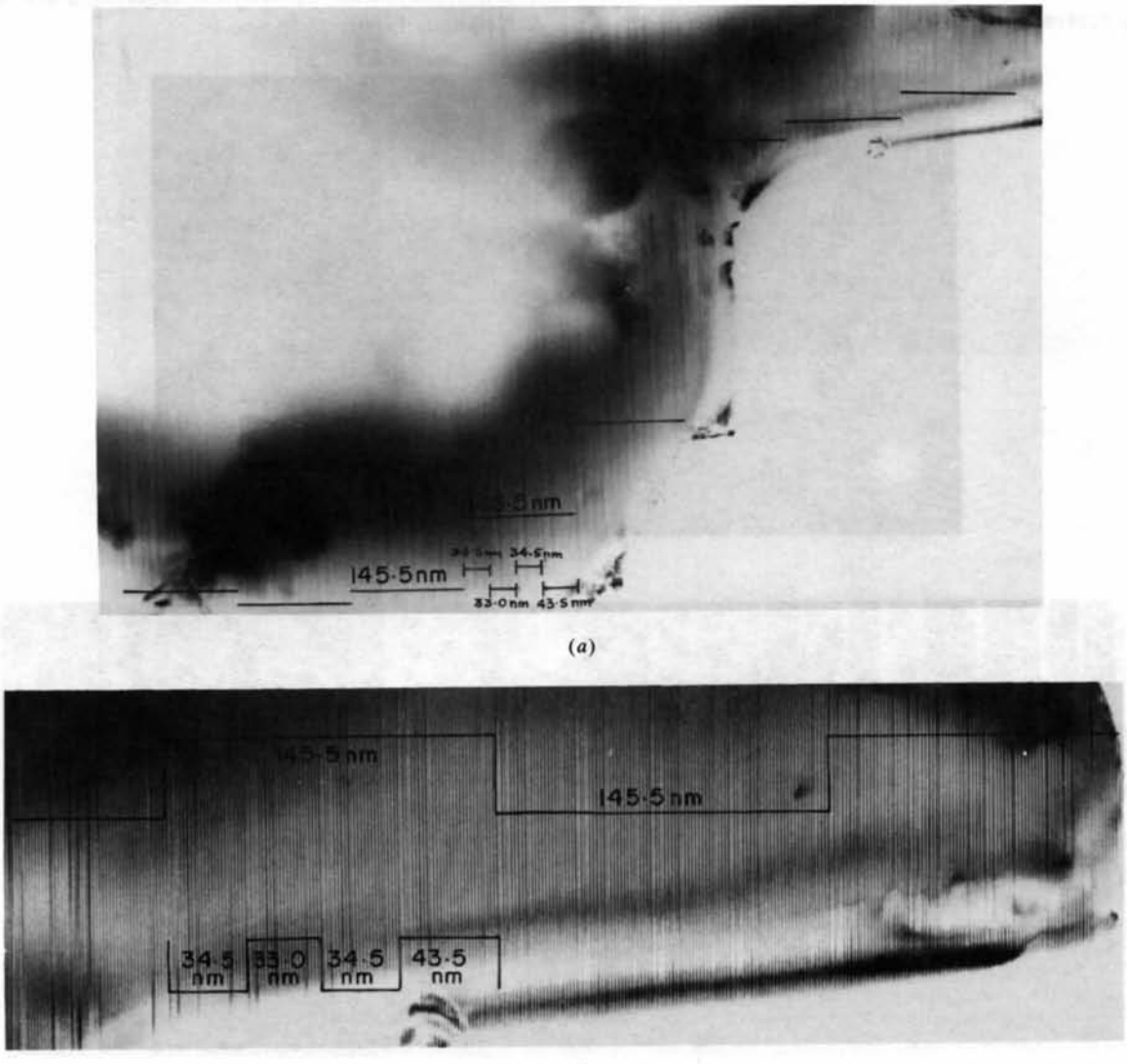

(*a*)

(*b*)

Fig. 4. (*a*) A bright-field lattice image, taken with symmetrical 000*l* reflections. Superperiod blocks of 145·5 nm periodicity are marked. Each block consists of intergrowth of 34·5, 33·0, 34·5 and 43·5 nm blocks. The 34·5 nm blocks correspond to the periodicity inferred from X-ray diffraction. (*b*) Enlargement of a portion of the bright-field lattice image (*a*) to show details of the intergrowth.

units like 43 (marked by arrows in Fig. 5*b*) are not manifested very clearly. Therefore, the structure was confirmed by establishing a match between observed and calculated X-ray intensities.

Structure determination of 411*R polytype*

The above structure has $n_+ - n_- \neq 3r$ (where n_+ represents the total number of layers in cyclic sequence, n_- the number in anticyclic sequence and r is any positive or negative integer including zero), which indicates that it is a rhombohedral structure (Verma & Krishna, 1966). Therefore, the layer sequence of this structure referred to the hexagonal cell is given as

$$\{32\ 23\ 33\ 22\ 23\ (33)_2\ 43\ 33\ 32\ (33)_9\ 22\ (33)_4\}_3.$$

This represents a 411*R* polytype structure.

To confirm a SiC polytype structure, it is sufficient to compare the calculated and observed X-ray intensities of the $10\bar{1}l$ row of reflections alone (Ramsdell, 1944; Verma & Krishna, 1966). Accordingly, the intensities of $10\bar{1}l$ reflections were calculated for this structure and a match between the calculated and visually observed X-ray intensities is given in Table 1. Although the full range of $10\bar{1}l$ reflections is not experimentally available owing to reasons discussed earlier, the match between the calculated and observed X-ray intensities for the available reflections is quite good. This amply confirms the structure which had already been read from the two-dimensional image with some reliability. The detailed atomic parameters for the structure {32 23 33 22 23 $(33)_2$ 43 33 32 $(33)_9$ 22 $(33)_4\}_3$ in Zhdanov notation may be obtained by the usual method (Verma & Krishna, 1966).

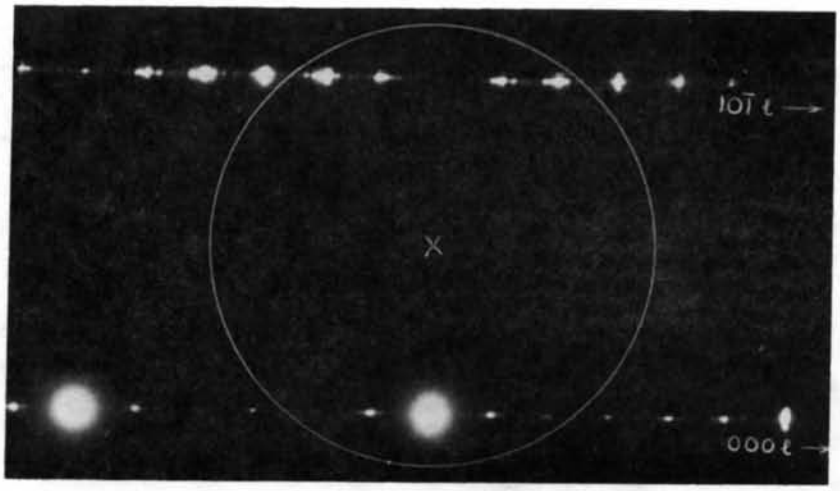

(*a*)

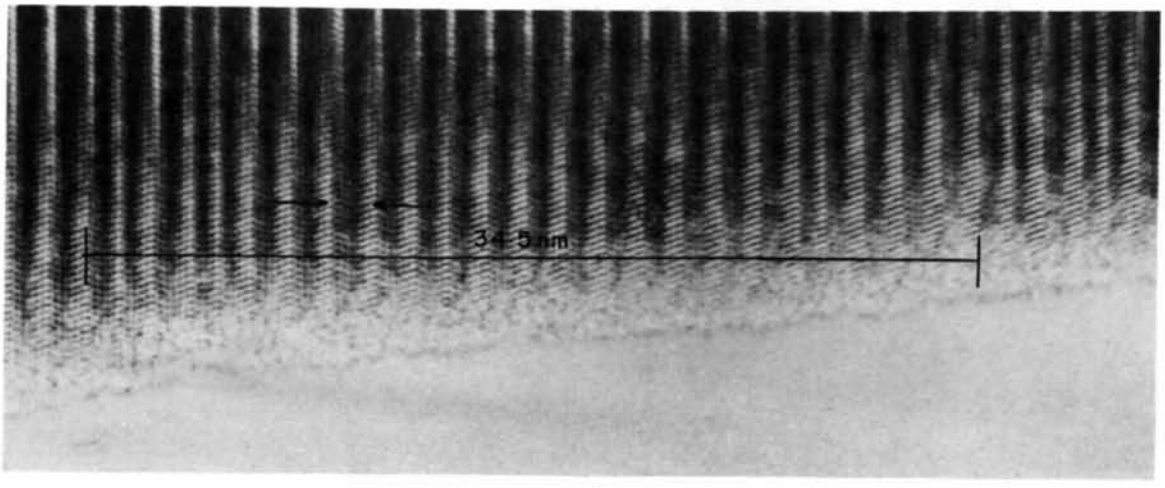

(*b*)

Fig. 5. (*a*) Electron diffraction pattern of the 411*R* polytype and its intergrowth structures. Positions of aperture and optic axis are marked. (*b*) Two-dimensional lattice image taken under tilted illumination of the same crystal showing one 34·5 nm wide block. Objective aperture symmetrically includes 000*l* and $10\bar{1}l$ reflections as shown in (*a*).

Table 1. *Calculated and observed X-ray intensities of the* 411*R structure*

$\bar{l}$ in $10\bar{1}l$	Calculated intensity	Observed intensity*	$\bar{l}$ in $10\bar{1}l$	Calculated intensity	Observed intensity*
2	3·2	*a*	143	66·7	*w*
5	6·7	*a*	146	560·9	*s*
8	97·4	*w*	149	124·5	*w*
11	62·1	*w*	152	14·8	*a*
14	4·8	*a*	155	0·8	*a*
17	24·9	*a*	158	85·6	*w*
20	23·9	*a*	161	30·8	*vw*
23	8·7	*a*	164	1·6	*a*
26	3·1	*a*	167	0·9	*a*
29	29·8	*vw*	170	29·4	*vw*
32	31·6	*vw*	173	31·0	*vw*
35	114·4	*w*	176	5·5	*a*
38	25·1	*a*	179	16·5	*a*
41	6·3	*a*	182	4·2	*a*
44	52·5	*vw*	185	11·1	*a*
47	98·5	*w*	188	10·6	*a*
50	46·5	*vw*	191	32·4	*vw*
53	38·6	*vw*	194	30·1	*vw*
56	12·5	*a*	197	57·6	*w*
59	608·3	*s*	200	115·0	*w*
62	351·4	*s*	203	340·5	*s*
65	667·6	*s*	206	2477·5	*vvs*
68	343·3	*s*	209	114·9	*w*
71	2115·9	*vvs*	212	140·8	*ms*
74	230·9	*ms*	215	32·4	*vw*
77	90·9	*w*	218	6·5	*a*
80	88·1	*w*	221	2·8	*a*
83	356·5	*s*	224	3·2	*a*
86	310·5	*s*	227	8·1	*a*
89	21·9	*a*	230	2·9	*a*
92	19·6	*a*	233	5·1	*a*
95	125·5	*w*	236	3·9	*a*
98	57·1	*vw*	239	8·8	*a*
101	62·7	*w*	242	3·8	*a*
104	81·4	*w*	245	4·1	*a*
107	22·6	*a*	248	5·4	*a*
110	96·9	*w*	251	10·1	*a*
113	13·1	*a*	254	34·1	*vw*
116	6·7	*a*	257	3·9	*a*
119	240·5	*ms*	260	3·3	*a*
122	490·0	*s*	263	77·1	*w*
125	175·4	*ms*	266	15·2	*a*
128	402·6	*s*	269	131·2	*ms*
131	249·5	*ms*	272	1·5	*a*
134	1790·4	*vs*	275	176·4	*ms*
137	1112·6	*vs*	278	495·2	*s*
140	1164·6	*vs*			

* *vvs, vs, s, ms, w, vw, a* stand for very very strong, very strong, strong, medium strong, weak, very weak and absent, respectively.

Intergrowth structures 519*R and* 393*R*

X-ray diffraction methods prove to be inadequate for detailed investigation of structures involving intergrowth at the unit-cell level. This is because X-ray diffraction methods yield only an average Patterson function (Cochran & Howells, 1954) which, although interpretable for simple structures, becomes exceedingly complex when more than one structure is intergrown coherently at microscopic level. Lattice imaging plays a complementary role in such situations (Singh & Singh, 1980; Singh *et al.*, 1981). It may be noted that a superperiod structure of 145·5 nm periodicity is built up of subunits of 43·5 and 33·0 nm in addition to those of 411*R*. Since it has been possible to derive the layer sequence of 411*R* units from the chevron-shaped fringes, the structures of other intergrowth units can also be reliably derived.

It can be seen from Fig. 4 that the layer sequence in the 43·5 nm block is similar to that of 411*R* except that it contains a block of 15 successive fringes of 6*H* periodicity in place of nine such fringes in the 411*R* unit cell and it is identified as a 519*R* structure. On the other hand, the 33·0 nm wide block has again a similar layer sequence to 411*R* except that it has eight successive fringes of 6*H* periodicity in place of nine in the 411*R* unit (Fig. 4) and therefore is identified as a 393*R* structure.

Superperiod structure 1734*R*

After decoding the layer sequence of constituent units, which intergrow coherently to form a superperiod structure, one can write the full layer sequence of this structure in Zhdanov notation as

$$[\{32\,23\,33\,22\,23\,(33)_2\,43\,33\,32\,(33)_9\,22\,(33)_4\}$$
$$\{32\,23\,33\,22\,23\,(33)_2\,43\,33\,32\,(33)_8\,22\,(33)_4\}$$
$$\{32\,23\,33\,22\,23\,(33)_2\,43\,33\,32\,(33)_9\,22\,(33)_4\}$$
$$\{32\,23\,33\,22\,23\,(33)_2\,43\,33\,32\,(33)_{15}\,22\,(33)_4\}].$$

This represents a rhombohedral structure having 1734 Si–C double layers in the hexagonal unit cell. Therefore, it is identified as 1734*R* and the complete structure is derived by repeating the above Zhdanov sequence three times.

Discussion and conclusion

It has been seen from the above example that tilted-beam two-dimensional lattice images taken under specific conditions contain direct information about the stacking sequence of layers in SiC structures. However, chevron-shaped fringes simulating the layer stacking sequences are found to be extremely sensitive to experimental parameters. Consequently, the derived structural information remains ambiguous unless confirmed by other means. The reason for this state of affairs basically lies in the limited number of reflections which have been used for obtaining these pictures.

In contrast to the chevron-shaped fringes, the linear fringes normal to the *c* axis arise essentially from interference of different reflections of individual reciprocal-lattice rows along c^* (like $000l$ or $10\bar{1}l$). An image formed by reflections of only one reciprocal-lattice row can give a one-dimensional projection of structure. In a low-resolution one-dimensional image it is out of the question to observe the projected structure on a line. However, fringe modulations do take place at spacings which correspond to periodicities of constituent intergrown units actually forming a large-period structure. Such fringe modulations occur at the level of 1·0 nm or more,

whereas the included reflections in the objective aperture go up to spatial frequencies of 0·25 nm or so. Therefore, series-truncation errors are comparatively less, making fringe separations less sensitive to foil-thickness variations at an appropriate defocus value. Thus, structural information available from one-dimensional fringes contains less details but is more reliable (Dubey & Singh, 1978; Singh & Singh, 1980; Singh *et al.*, 1981; Yessik *et al.*, 1975; Ogbuji *et al.*, 1981; Kuo *et al.*, 1982). Therefore, wherever possible, a combination of linear fringe spacings and chevron-shaped fringes should be utilized to derive the structural information.

Ideally the structure–image correlation should be based on a thorough study of the variation of image contrast with crystal thickness, orientation, lens defocus and other aberrations. However, as pointed out earlier, such a study becomes impractical in large-period polytypes, making it imperative to depend on collaborative evidence as has been done in this investigation.

The four intergrown units forming the superperiod (Fig. 4) show a curious correlation with four cooperating spirals observed on the growth face (0001) of this crystal (Fig. 6). Although the step heights could not be measured by multiple-beam interferometry, the correlation between four spirals with four structural subunits in the superperiod tentatively suggests that the superperiod structure was formed by a screw dislocation mechanism.

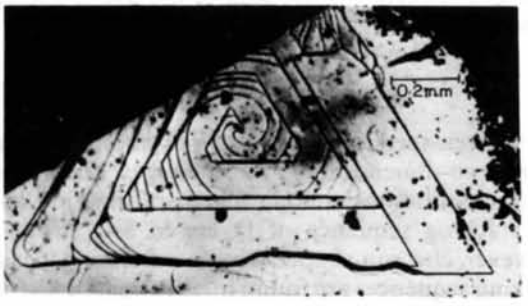

Fig. 6. Optical micrograph of (0001) face of the same crystal (411*R* and its intergrowth structures) showing four cooperating spiral ledges. All the spirals originate from the centre.

We are grateful to Professor K. H. Jack, FRS, of the Crystallography Laboratory, University of Newcastle Upon Tyne, England, for his encouragement and for providing the experimental facility of JEM 100 CX for this work. One of us (RSR) is grateful to DST, India, for financial assistance during the tenure of the present work.

References

ALLPRESS, J. G. & SANDERS, J. V. (1973). *J. Appl. Cryst.* **6**, 165–190.
BUSECK, P. R. & IIJIMA, S. (1974). *Am. Mineral.* **59**, 1–21.
COCHRAN, W. & HOWELLS, E. R. (1954). *Acta Cryst.* **7**, 412–415.
COWLEY, J. M. & IIJIMA, S. (1972). *Z. Naturforsch. Teil A*, **27**, 445–451.
COWLEY, J. M. & MOODIE, A. F. (1957). *Acta Cryst.* **10**, 609–619.
DUBEY, M., RAM, U. S. & SINGH, G. (1973). *Acta Cryst.* B**29**, 1548–1550.
DUBEY, M. & SINGH, G. (1978). *Acta Cryst.* A**34**, 116–120.
GOODMAN, P. & MOODIE, A. F. (1974). *Acta Cryst.* A**30**, 280–290.
HASHIMOTO, H., ENDOH, H., TAKAI, Y., TOMIOKA, H. & YOKOTA, Y. (1978/79). *Chem. Scr.* **14**, 23–31.
JEPPS, N. W., SMITH, D. J. & PAGE, T. F. (1979). *Acta Cryst.* A**35**, 916–923.
KUO, C. L., ZHOU, J., YE, H. Q. & KUO, K. H. (1982). *J. Appl. Cryst.* **15**, 199–205.
MCCONNELL, J. D. M., HUTCHISON, J. L. & ANDERSON, J. S. (1974). *Proc. R. Soc. London Ser. A*, **339**, 1–12.
OGBUJI, L. U., MITCHELL, T. E. & HEUER, A. H. (1981). *J. Am. Ceram. Soc.* **64**, 91–99.
RAMSDELL, L. S. (1944). *Am. Mineral.* **29**, 431–442.
SINGH, S. R. & SINGH, G. (1980). *Acta Cryst.* A**36**, 779–784.
SINGH, S. R., SINGH, G. & VAN TENDELOO, G. (1981). *Phys. Status Solidi A*, **67**, 625–632.
SKARNULIS, A. J. (1976). PhD Thesis, Arizona State Univ.
SMITH, D. J. & O'KEEFE, M. A. (1983). *Acta Cryst.* A**39**, 139–148.
VAN LANDUYT, J., AMELINCKX, S., KOHN, J. A. & ECKART, D. W. (1974). *J. Solid State Chem.* **9**, 103–119.
VAN TENDELOO, G. & AMELINCKX, S. (1982). *Phys. Status Solidi A*, **69**, 103–120.
VERMA, A. R. & KRISHNA, P. (1966). *Polymorphism and Polytypism in Crystals.* New York: John Wiley.
YESSIK, M., SHINOZAKI, S. & SATO, H. (1975). *Acta Cryst.* A**31**, 764–768.